

A Novel Methodology for Robust Dynamic Positioning of Marine Vessels: Theory and Experiments*

Vahid Hassani¹, Asgeir J. Sørensen² and António M. Pascoal³

Abstract—The paper describes a novel robust adaptive controller for Dynamic Positioning (DP) of marine vessels. The proposed Robust Multiple Model Adaptive Dynamic Positioning (RMMADP) structure consists of a bank of robust controllers designed using the Mixed- μ methodology and an identification unit. The latter is composed by a bank of (steady-state) Kalman filters (KFs) that generate online the output estimation errors (residuals) that are used to generate appropriate monitoring signals. At each sampling time, the monitoring signals are assessed to decide which controller should be selected from the bank of the controllers. The proposed adaptive structure of the RMMADP enables the DP system to operate in different operational conditions and hence, it is a step forward to a so-called all-year marine DP system. Numerical simulations, carried out with a high fidelity nonlinear DP simulator, illustrate the efficacy of the RMMADP techniques proposed. To bridge the gap between theory and practice, the results are experimentally verified by model testing a DP operated ship, the Cybership III, under different sea conditions in a towing tank equipped with a hydraulic wave maker.

I. INTRODUCTION

The first generation of DP systems came to existence in the 1960s for offshore drilling applications, due to the need to drill in deep waters and the realization that Jack-up barges and anchoring systems could not be used economically at such depths. The first vessel equipped with a Dynamic Positioning (DP) system was launched in 1961 [1]. The vessel, named Eureka, was property of the Shell Oil Company. Nowadays, DP systems are used with a wide range of vessel types and in different marine operations such as hydrographic surveying, marine construction, wreck investigation, underwater recovery, site surveying, underwater cable and pipe laying, and inspection and maintenance. In particular, in the offshore, oil, and gas industries many applications are only possible with the use of DP systems for service vessels, drilling rigs and ships, shuttle tankers, cable and pipe layers, floating production off-loading and storage units (FPSOs),

*This work was supported in part by projects MORPH (EU FP7 under grant agreement No. 288704) and PESt-OE/EEI/LA0009/2011, and was carried out in cooperation with the Norwegian Marine Technology Research Institute (MARINTEK) and the Centre for Autonomous Marine Operations and Systems (AMOS); the Norwegian research council is acknowledged as sponsor of MARINTEK and AMOS.

¹Vahid Hassani was formerly with LARSyS, Portugal, and is now with the Norwegian Marine Technology Research Institute (MARINTEK), Trondheim, Norway. vahid.hassani@marintek.sintef.no

²A. J. Sørensen is with Centre for Autonomous Marine Operations and Systems (AMOS) and Dept. of Marine Technology, Norwegian Univ. of Science and Technology, Trondheim, Norway. asgeir.sorensen@ntnu.no

³António M. Pascoal is with the Laboratory of Robotics and Systems in Engineering and Science (LARSyS), Instituto Superior Técnico (IST), Univ. Técnica de Lisboa (UTL), Lisbon, Portugal. antonio@isr.ist.utl.pt

crane and heavy lift vessels, geological survey vessels, and multi-purpose supply and intervention vessels.

Early dynamic positioning systems were implemented using PID controllers. In order to restrain thruster trembling caused by the wave-induced motion components, notch filters in cascade with low pass filters were used with the controllers. An improvement in performance was achieved by exploiting more advanced control techniques based on optimal control and Kalman filter theory, see [2]–[4]. A simpler set-up based on nonlinear passive observers (to replace Kalman filters) was introduced in [5]–[7]. Further developments in recent years have led to the use of nonlinear control [8], robust control [9], [10], adaptive control [11] and hybrid control [12] theories in the design of DP systems. The literature on ship DP is vast and defies a simple summary. See for example [13], [14] and the references therein for a short presentation of the subject and its historical evolution.

Most of the current DP systems are designed to operate up to certain limits of weather conditions. However, in practice the sea state may undergo large variations and therefore the controller should adapt to the sea state itself. To meet this challenge, different techniques have been proposed. Among them, supervisory control techniques were exploited in [12] to design a hybrid DP controller. A distinctive feature of the controller developed was the use of spectral techniques to estimate the wave spectrum in surge, sway, and yaw from position and heading measurements. The results were used to identify the sea state, based on which the appropriate controller was selected from a pre-defined bank of controllers. However, this approach is sensitive to measurement noise and may have latency problems because it requires that the samples acquired be buffered to estimate the Power Density Spectrum of the measurement time series.

In this paper, availing ourselves of previous results obtained by the authors in [9], [10], [15], [16], we propose a new type of DP control law that we will henceforth be referred to as a Robust Multiple Model Adaptive Dynamic Positioning (RMMADP) system. A bank of individual robust DP controllers for different sea conditions (calm, moderate, high and extreme) are designed using mixed- μ techniques [17]. In the new structure proposed, a bank of Kalman filters are designed based on a finite number of models of the vessel when it undergoes operations under different sea conditions. Multiple model identification tools are used to identify the sea state and to select the appropriate (locally) robust DP controller from a pre-defined bank of the controllers. The main objective of this paper is to integrate a bank of appropriate robust DP controllers into a state-of-the-art robust adaptive DP architecture yielding good performance

in varying operational conditions, from calm to extreme seas. The proposed structure extends the so-called weather window operational availability of a DP system without the need for spectral identification techniques (which exhibit latency and are very sensitive to measurement noise).

Numerical simulations, carried out in a high fidelity non-linear DP simulator, illustrate the efficacy of the RMMADP techniques proposed. To bridge the gap between theory and practice, the results are experimentally verified by model testing of a DP operated ship, the Cybership III, under different simulated sea conditions in a towing tank equipped with a hydraulic wave maker.

The structure of the paper is as follows. In section II we present the main issues that arise in the design of the RMMADP. In Section III we present the results of numerical Monte-Carlo simulations with stochastic signals, carried out in the Marine Cybernetics Simulator, that illustrate the performance of developed DP controller in calm to extreme sea conditions. In section IV, a short description of the model-test vessel, Cybership III, and experimental results of model-tests are presented. Conclusions and suggestions for future research are summarized in Section V.

II. THE ROBUST MULTIPLE-MODEL ADAPTIVE DYNAMIC POSITIONING

In what follows, the vessel model that is by now standard¹ is presented. See for example [6], [8], [18], [19]. The model admits the realization

$$\dot{\xi}_W = A_W(\omega_0)\xi_W + E_W w_W \quad (1)$$

$$\eta_W = R(\psi_L)C_W\xi_W \quad (2)$$

$$\dot{b} = -T^{-1}b + E_b w_b \quad (3)$$

$$\dot{\eta}_L = R(\psi_L)\nu \quad (4)$$

$$M\dot{\nu} + D\nu = \tau + R^T(\psi_{tot})b \quad (5)$$

$$\eta_{tot} = \eta_L + \eta_W \quad (6)$$

$$\eta_y = \eta_{tot} + v, \quad (7)$$

where (1) and (2) capture the 1st-order wave induced motions in surge, sway, and yaw; equation (3) represents the 1st-order Markov process approximating the unmodelled dynamics and the slowly varying environmental forces (in surge and sway) and torques (in yaw) due to waves (2nd order wave induced loads), wind, and currents. The latter are given in earth fixed coordinates but expressed in body-axis. In the above, $\eta_W \in \mathbb{R}^3$ is the vessel's WF motion due to 1st-order wave-induced disturbances, consisting of WF position (x_W, y_W) and WF heading ψ_W of the vessel; $w_W \in \mathbb{R}^3$ and $w_b \in \mathbb{R}^3$ are zero mean Gaussian white noise vectors, and

$$A_W = \begin{bmatrix} 0_{3 \times 3} & I_{3 \times 3} \\ -\Omega_{3 \times 3} & -\Lambda_{3 \times 3} \end{bmatrix}, \quad E_W = \begin{bmatrix} 0_{3 \times 1} \\ I_{3 \times 1} \end{bmatrix},$$

$$C_W = \begin{bmatrix} 0_{3 \times 3} & I_{3 \times 3} \end{bmatrix},$$

¹The model described by (1)-(6) has minor differences with respect to the ones normally available in the literature. While in most of the literature the WF components of motion are modeled in a fixed-earth frame, in this paper the WF motion is modeled in body-frame. The reader is referred to [16], [20] for details and improvements of the present model.

with

$$\Omega = \text{diag}\{\omega_{01}^2, \omega_{02}^2, \omega_{03}^2\},$$

$$\Lambda = \text{diag}\{2\zeta_1\omega_{01}, 2\zeta_2\omega_{02}, 2\zeta_3\omega_{03}\},$$

where $\omega_0 = [\omega_{01} \ \omega_{02} \ \omega_{03}]^T$ and ζ_i are the Dominant Wave Frequency (DWF) and relative damping ratio, respectively. Matrix $T = \text{diag}(T_x, T_y, T_\psi)$ is a diagonal matrix of positive bias time constants and $E_b \in \mathbb{R}^{3 \times 3}$ is a diagonal scaling matrix. Vector $\eta_L \in \mathbb{R}^3$ consists of low frequency (LF), earth-fixed position (x_L, y_L) and LF heading ψ_L of the vessel relative to an earth-fixed frame, $\nu \in \mathbb{R}^3$ represents the velocities decomposed in a vessel-fixed reference, and $R(\psi_L)$ is the standard orthogonal yaw angle rotation matrix (see [21] for complete details). Equation (5) describes the vessels's LF motion at low speed (see [21]), where $M \in \mathbb{R}^{3 \times 3}$ is the generalized system inertia matrix including zero frequency added mass components, $D \in \mathbb{R}^{3 \times 3}$ is the linear damping matrix, and $\tau \in \mathbb{R}^3$ is a control vector of generalized forces generated by the propulsion system, that is, the main propellers aft of the ship and thrusters which can produce surge and sway forces as well as a yaw moment. Vector $\eta_{tot} \in \mathbb{R}^3$ describes the vessel's total motion, consisting of total position (x_{tot}, y_{tot}) and total heading ψ_{tot} of the vessel. Finally, (7) represents the position and heading measurement equation, with $v \in \mathbb{R}^3$ a zero-mean Gaussian white measurement noise.

From (1)-(6), using practical assumptions, a linear model with parametric uncertainty was obtained in [9] as follows:

$$\dot{\xi}_W = A_W(\omega_0)\xi_W + E_W w_W \quad (8)$$

$$\eta_W^b = C_W\xi_W \quad (9)$$

$$\dot{b}^p = -T^{-1}b^p + \theta_1 S b^p + w_b^f \quad (10)$$

$$\dot{\eta}_L^p = \theta_1 S \eta_L^p + \nu + \theta_2 S \nu \quad (11)$$

$$M\dot{\nu} + D\nu = \tau + b^p \quad (12)$$

$$\eta_y^f = \eta_L^p + \eta_W^b + n \quad (13)$$

where η_W^b are WF components of motion on the body-coordinate axis, w_b^f and η_y^f are a new modified disturbance and a modified measurement defined by $w_b^f = R^T(\psi_y)E_b w_b$ and $\eta_y^f = R^T(\psi_y)\eta_{tot} + n$, respectively, $n \in \mathbb{R}^3$ is the measurement noise, ω_0 , θ_1 , and θ_2 are parametric uncertainties given in Table II, and the matrix S is given by

$$S = \begin{bmatrix} 0 & 1 & 0 \\ -1 & 0 & 0 \\ 0 & 0 & 0 \end{bmatrix}.$$

The equations describing the kinematics and the dynamics of the vessel can be represented in the following standard form for multiple-input-multiple-output (MIMO) linear plant models:

$$\dot{x}(t) = A(\omega_0, \theta_1, \theta_2)x(t) + Bu(t) + Lw(t), \quad (14a)$$

$$y(t) = Cx(t) + v(t), \quad (14b)$$

where $x(t) = [\xi_W^T \ b^p{}^T \ \eta_L^p{}^T \ \nu^T]^T \in \mathbb{R}^{15}$ denotes the state of the system, $u(t) = M^{-1}\tau \in \mathbb{R}^3$ its control input, $y(t) = \eta_y^f \in \mathbb{R}^3$ its measured noisy output, $w(t) =$

$[w_W^T w_b^T]^T \in \mathbb{R}^6$ an input plant disturbance that cannot be measured, and $v(t) = n \in \mathbb{R}^3$ is the measurement noise. The equations in (14) are simply a compact way of presenting equations in (8)-(13); $A(\omega_0, \theta_1, \theta_2)$, B , L and C are defined in the obvious manner. Vectors $w(t)$ and $v(t)$ are zero-mean white Gaussian signals, mutually independent with intensities $E\{w(t)w^T(\tau)\} = Q\delta(t - \tau)$ and $E\{v(t)v^T(\tau)\} = R\delta(t - \tau)$. The initial condition $x(0)$ of (14) is a Gaussian random vector with mean and covariance given by $E\{x(0)\} = 0$ and $E\{x(0)x^T(0)\} = \Sigma(0)$, respectively. Matrix $A(\omega_0, \theta_1, \theta_2)$ contains *unknown constant parameters* indexed by ω_0 , θ_1 , and θ_2 . The parametric uncertainty interval of θ_1 and θ_2 is very small¹ and the main parametric uncertainty in the the model given by (14) is the DWF, ω_0 . Table I shows the definition of the sea conditions characterized by the DWF. The sea conditions are associated with the particular model of offshore supply vessel that is used in our study. We assume that DWF lies in the interval

TABLE I
DEFINITION OF SEA STATES FROM [22]

Sea States	DWF ω_0 (rad/s)	Significant Wave Height H_s (m)
Calm Seas	> 1.11	< 0.1
Moderate Seas	$[0.74 \ 1.11]$	$[0.1 \ 1.69]$
High Seas	$[0.53 \ 0.74]$	$[1.69 \ 6.0]$
Extreme Seas	< 0.53	> 6.0

TABLE II
INTERVAL OF PARAMETRIC UNCERTAINTIES

Sea Status	ω_0 rad/s	θ_1 rad/s ²	θ_2 rad/s
Calm Seas	$[1.11 \ 1.8]$	Int*	$[-0.038 \ 0.038]$
Moderate Seas	$[0.74 \ 1.11]$	Int	$[-0.04 \ 0.04]$
High Seas	$[0.53 \ 0.74]$	Int	$[-0.042 \ 0.042]$
Extreme Seas	$[0.39 \ 0.53]$	Int	$[-0.04 \ 0.04]$

* Int= $[-5 \times 10^{-4} \ 5 \times 10^{-4}]$

$[0.39 \ 1.8]^2$ that covers calm, moderate, high and extreme sea conditions.

In the RMMADP deign methodology we divide the parametric uncertainty region into smaller regions and we design robust controllers K_i for each subregion, using the μ -synthesis method [17], [23]. Here, we borrow from the work in [9], [10] where four (locally) robust DP controllers, for calm, moderate, high and extreme sea conditions, were designed and their performance evaluated both through numerical simulations (in the Marine Cybernetics Simulator - MCSim), and experimentally, performing model test experiments. Moreover, the performance of the designed robust DP controllers for different sea conditions is compared with the ones of LQG and PID controllers in [24] showing the satisfactory performance of robust DP controllers in different

sea conditions; in particular, superior performance of robust DP controllers in extreme sea condition is shown in [24].

In a RMMADP system a bank of KFs are used in order to select the correct controllers from the bank of the controllers. Each KF is designed based on a selected value of the unknown parameter, ω_0 . The residuals of all the KFs are analyzed in a block called Monitoring Signal Evaluator (MSE). The MSE assigns a performance index (monitoring signal) to each KF (and the corresponding controller). Then, the monitoring signals μ_i (to be defined shortly) are associated with the i^{th} KF (and i^{th} controller, i.e. K_i , in the bank of the controllers). These monitoring signals are used to select the best local controller from the bank of robust DP controllers. Four selected values for ω_0 are chosen as $\{0.48, 0.63, 0.92, 1.18\}$ (rad/s). Each selected value represents one of the sea states, calm, moderate, high and extreme. The bank of the Kalman filters is designed based on the selected nominal values for the dominant wave frequency (DWF); see [24] for details on the design of a Kalman filter for DP systems and [25] for details on the selection of the nominal design models. Each steady state KF has the following realization [26]:

$$\begin{aligned} \hat{x}_i(t+1) &= A(\omega_0, \theta_1, \theta_2)\hat{x}_i(t) + Bu(t) + H_{\theta_i}(y(t) - \hat{y}_i(t)), \\ \hat{y}_i(t) &= C\hat{x}_i(t), \end{aligned}$$

$$H_{\theta_i} = A(\omega_0, \theta_1, \theta_2)P_iC^T[CP_iC^T + R]^{-1},$$

where P_i is the solution of the discrete Riccati equation

$$\begin{aligned} P_i &= A(\omega_0, \theta_1, \theta_2)P_iA(\omega_0, \theta_1, \theta_2)^T + LQL^T \\ &\quad - A(\omega_0, \theta_1, \theta_2)P_iC^T[CP_iC^T + R]^{-1}CP_iA(\omega_0, \theta_1, \theta_2)^T. \end{aligned} \quad (16)$$

It is assumed that $[A(\omega_0, \theta_1, \theta_2), L]$ and $[A(\omega_0, \theta_1, \theta_2), C]$ are controllable and observable, respectively for all admissible values of ω_0 , θ_1 , and θ_2 . The symmetric positive definite matrices Q and R were defined before as covariance matrices of the plant disturbance and measurement noise, respectively.

The output estimation errors ($\tilde{y}_i(t) = y(t) - \hat{y}_i(t)$) and error covariances of all the Kalman filters ($S_i = CP_iC^T + R$) are used to compute a performance signal that can be viewed as a gaussian maximum likelihood ratio. This signal is called a "monitoring signal" $\mu_i(t)$, and is defined as

$$\mu_i(t) := \frac{1}{t} \sum_{k=1}^t \frac{1}{2} \tilde{y}_i(k)^T S_i^{-1} \tilde{y}_i(k) + \ln((2\pi)^{\frac{3}{2}} \sqrt{|S_i|}). \quad (17)$$

For more details on definition and concept of the monitoring signals see [15]. The monitoring signals are then used to select one of the local controllers (the one associated with Kalman filter with the smallest monitoring signal).

Fig. 1 shows the architecture of the RMMADP system. The RMMADP, in Fig. 1, consists of: i) the monitoring signal evaluator, ii) a bank of N KFs, where each local estimator is designed based on one of the representative parameters, and iii) a bank of N robust DP controllers which are switched in the feedback loop based on the values of monitoring signals. A dwell-time switching policy is used to prevent chattering

¹See [5]–[7] where θ_1 and θ_2 are ignored in the design process.

²We use the same interval for DWF in surge, sway and yaw.

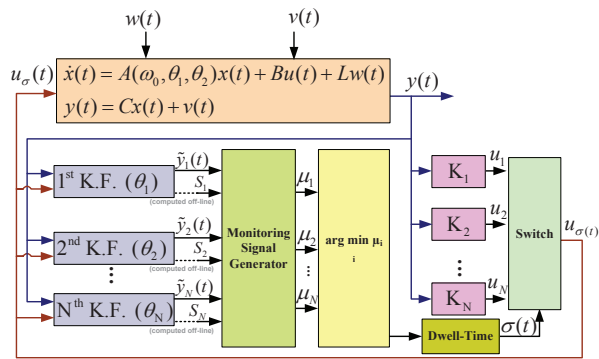


Fig. 1. The RMMADP architecture.

among the controllers, see [15] for details on the structure of the RMMADP. The stability of the overall system is studied in [15]. It is shown that in steady state the correct controller is selected and during the transient all the internal signals remain bounded. The control action is $u_\sigma(t)$, where $\sigma = \operatorname{argmin}\{\mu_i(t)\}$.³

In DP systems, it is important that the controller adapt to the sea state that may change during operations. In the RMMADP methodology, in order to distinguish the sea state, a multiple model structure is exploited to identify the sub-interval that the peak frequency of the assumed wave spectrum model lies in. Based on the results of the identification, which are carried out at each sampling time by assessing the monitoring signals, an appropriate controller (from the bank) is switched in the feedback loop.

III. NUMERICAL SIMULATIONS

In what follows we test the performance of our controller using the Marine Cybernetics Simulator (MCSim), later on upgraded to the Marine System Simulator (MSS). The MCSim is a modular multi-disciplinary simulator based on Matlab/Simulink. It was developed at the department of marine technology of the Norwegian University of Science and Technology (NTNU). The MCSim incorporates high fidelity models, denoted as process plant model or simulation model in [19], at all levels (plants and actuators). It captures hydrodynamic effects, generalized coriolis and centripetal forces, nonlinear damping and current forces, and generalized restoring forces. It is composed of different modules such as environmental module, vessel dynamics module, thruster and shaft module, and Vessel control module. For more details on the MCSim see [27], [28].

The results of Monte-Carlo simulations aimed at assessing the performance of the RMMADP controller are presented below. In these simulations, the different environment conditions from calm to extreme seas are simulated using the spectrum of the Joint North Sea Wave Project (JONSWAP) [29]. Throughout the paper, four different environment conditions from calm to extreme seas are considered. Table I

³In this architecture, the identification module (that relies on monitoring signal evaluator) computes the smallest monitoring signal μ_i ; $i \in \{1, 2, \dots, N\}$ and switches the controller K_i associated with that monitoring signal, after which it dwells on that selection for a predefined time, called dwell-time. See [15] for details on dwell-time and how to compute it.

shows the definition of the sea condition associated with a particular model of supply vessel that is used in the MCSim. The sampling time of $T_s = .25$ (sec) is used to implement the RMMADP system throughout the simulation and experimental tests.

Fig. 2 shows the results of a simple simulation⁴. In this experiment we examine the performance of the RMMADP system in different sea conditions. The first (upper) sub-figure shows the switching signal in a calm sea condition. The second sub-figure shows the switching signal in a moderate sea condition. The switching signal in high sea condition is shown in the third sub-figure and finally the switching signal in extreme sea state is depicted in the last (lowest) sub-figure of Fig. 2.

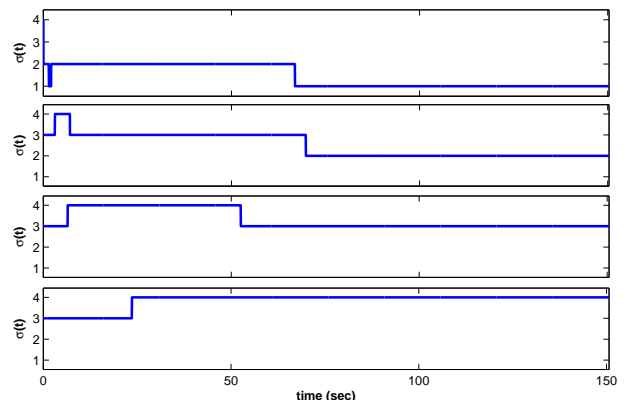


Fig. 2. Simulation result: Switching signals in different sea conditions; from top to bottom: calm, moderate, high, and extreme sea condition.

We stress that the performance of any adaptive system must be evaluated not only for constant unknown parameters but also, for time-varying parameters which undergo slow or rapid time-variations. In practice, the sea state may experience large variations and therefore adaptation is necessary in the dynamic positioning. Fig. 3 shows the results of the simulation where the sea state changes in time. In this experiment, during the first 300 seconds the moderate sea state is simulated and for the next 300 seconds the sea state changes to high condition. Fig. 3 represents the time evolution of the switching signal and the position of the vessel. The first sub-figure shows the switching signal; clearly RMMADP system follows the sea changes.⁵ The remaining sub-figures in Fig. 3 depicts the time evolution of the position of the vessel.

IV. EXPERIMENTAL RESULTS

The controller designed was tested using the model vessel Cybership III, at the Marine Cybernetic Laboratory (MCLab)

⁴All the results in the paper are presented in full scale.

⁵For the time varying case, 2 monitoring signals are computed for each observer. The monitoring signals reset every 40 seconds (with a 20 second time difference between the resetting time of the monitoring signals associated with each observer) and at each time only one of these monitoring signals (for each observer) goes to the supervisor. This means that when a monitoring signal, which is fed to supervisor, resets its value, the other monitoring signal whose value was reset 20 seconds ago and has by now reached its steady state value, will be fed to the supervisor.

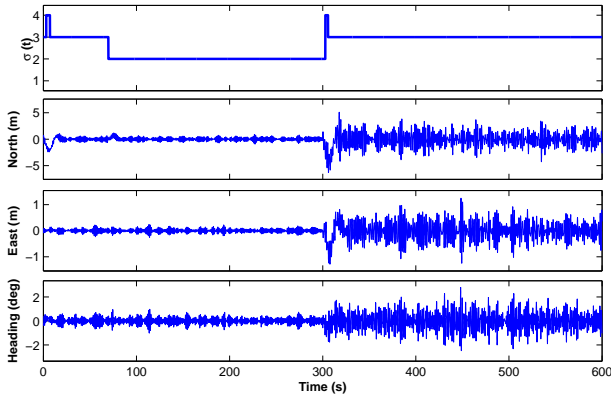


Fig. 3. Simulation result: Evolution of the switching signal and the position of the vessel in a time varying scenario

of the Department of Marine Technology at the Norwegian University of Science and Technology (NTNU). The performance of the controllers was tested under different sea conditions produced by a hydraulic wave maker.

A. Overview of the Cybership III

CyberShip III is a 1:30 scaled model of an offshore vessel operating in the North Sea. Fig. 4 shows the vessel at the basin in the MCLab and table III presents the main parameters of the model and full scale vessel.

TABLE III
MODEL MAIN PARAMETERS

	Model	Full Scale
Overall Length	2.275 m	68.28 m
Length between perpendiculars	1.971 m	59.13 m
Breadth	0.437 m	13.11 m
Breadth at water line	0.437 m	13.11 m
Draught	0.153 m	4.59 m
Draught front perpendicular	0.153 m	4.59 m
Draught aft. perpendicular	0.153 m	4.59 m
Depth to main deck	0.203 m	6.10 m
Weight (hull)	17.5 kg	Unknown
Weight (normal load)	74.2 kg	22.62 tons
Longitudal center of gravity	100 cm	30 m
Vertical center of gravity	19.56 cm	5.87 m
Propulsion motors max shaft power (6% gear loss)	81 W	3200 HP
Tunnel thruster max shaft power (6% gear loss)	27 W	550 HP
Maximum Speed	Unknown	11 knots



Fig. 4. Cybership III.

Cybership III is equipped with two pods located at the aft. A tunnel thruster and an azimuth thruster are installed in the

bow.⁶ It has a mass of $m = 75$ (kg), length of $L = 2.27$ (m) and breadth of $B = 0.4$ (m). Main parameters of the model is presented in Table III. The internal hardware architecture is controlled by an onboard computer which can communicate with onshore PC through a WLAN. The PC onboard the ship uses QNX real-time operating system (target PC). The control system is developed on a PC in the control room (host PC) under Simulink/Opal and downloaded to the target PC using automatic C-code generation and wireless Ethernet. The motion capture unit (MCU), installed in the MCLab, provides Earth-fixed position and heading of the vessel. The MCU consists of 3 onshore cameras mounted on the towing carriage and a marker mounted on the vessel. The cameras emit infrared light and receive the light reflected from the marker.

To simulate the different sea conditions, a hydraulic wave maker system was used. It consists of a single flap covering the whole breadth of the basin, and a computer controlled motor moving the flap. It can produce regular and irregular waves with different spectrums. We have used the JONSWAP spectrum to simulate the different sea conditions for our experiment.

Fig. 5 shows the results of the experiment where the wave maker system simulates different sea state conditions. Since the robust DP controllers are designed for a linearized system, a simple PI controller is used as an initializer to bring the vessel to the desired point (the origin) in the basin. The first (upper) sub-figure shows the wave elevation profile recorded by a probe installed five meters away from the wave maker. The second sub-figure shows the switching signal. As in the case of simulations, the RMMADP system keeps track of the sea state. However, we should stress that we have tuned the RMMADP during a few tests and Fig. 5 shows the final tuned system. We also should highlight that the wave profiles generated by the wave maker for high and extreme seas were not very different due to the limited capacity of the wave maker. Therefore, identifying the high and extreme sea conditions proved to be more difficult than identifying the other conditions. The remaining sub-figures in Fig. 5 shows the time evolution of the position and heading of the vessel.

V. CONCLUSIONS AND FUTURE RESEARCH

A Robust Multiple Model Adaptive Dynamic Positioning (RMMADP) system was described. The RMMADP system can operate in time-varying operational conditions, from calm to extreme seas, thus making it a good candidate for all-year operations. Furthermore, the system dispenses with the need for spectral identification techniques (which exhibit delays and are very sensitive to measurement noise). The proposed RMMADP design built upon recent developments on robust adaptive techniques using a multiple model structure. The RMMADP consists of a bank of robust controllers designed using Mixed- μ methodology and an identification unit. The identification unit uses a bank of (steady-state) Kalman filters (KFs) that generates online appropriate monitoring signals. At each sampling time, the monitoring signals

⁶For technical reasons in this experiment the tunnel thruster was deactivated.

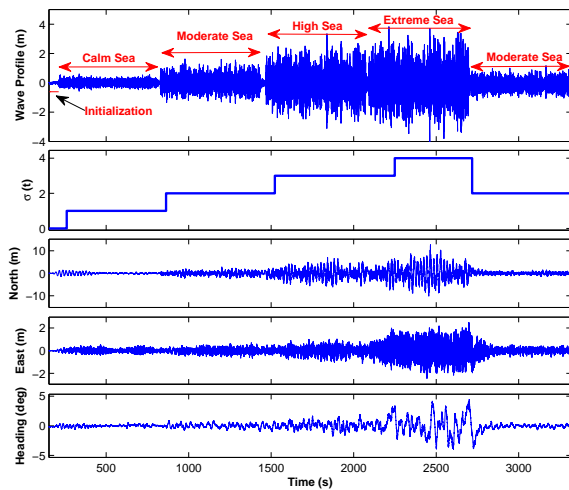


Fig. 5. Experimental results: evolution of the wave profile, the switching signal and the position of the vessel in time varying scenario (data is scaled from model to full scale).

are processed to select which controller should be selected from the bank of controllers. Numerical simulations, carried out with a high fidelity nonlinear DP simulator illustrated the efficacy of the RMMADP techniques proposed. The results were experimentally verified by model testing a DP operated ship, the Cybership III, under different simulated sea conditions in a towing tank with a hydraulic wave maker. The experimental data confirms that the method developed holds promise for practical applications.

ACKNOWLEDGMENT

We thank our colleagues A. Pedro Aguiar, J. Hespanha and Michael Athans for many discussions on adaptive control. We would also like to thank T. Wahl, Øyvind Smogeli, M. Etemaddar, E. Peymani, M. Shapouri, and B. Ommani for their great assistance during the model tests at MCLab.

REFERENCES

- [1] D. Bray, *Dynamic Positioning*, 2nd ed., ser. Oilfield Seamanship Series. London, UK: Oilfield Publications Ltd (OPL), 2003, vol. 9.
- [2] J. Balchen, N. Jenssen, and S. Sælid, "Dynamic positioning using Kalman filtering and optimal control theory," in *the IFAC/IFIP Symposium On Automation in Offshore Oil Field Operation*, Bergen, Norway, 1976, pp. 183–186.
- [3] M. J. Grimble, R. J. Patton, and D. A. Wise, "The design of dynamic ship positioning control systems using extended Kalman filtering techniques," in *Proc. IEEE Oceans Conference (Oceans'79)*, San Diego, CA, 1979, pp. 488–497.
- [4] S. Sælid, N. A. Jenssen, and J. Balchen, "Design and analysis of a dynamic positioning system based on Kalman filtering and optimal control," *IEEE Transactions on Automatic Control*, vol. 28, no. 3, pp. 331–339, 1983.
- [5] J. P. Strand, "Nonlinear position control systems design for marine vessels," Ph.D. dissertation, Dept. of Eng. Cybernetics, Norwegian University of Science and Technology, Trondheim, Norway, 1999.
- [6] J. P. Strand and T. I. Fossen, "Nonlinear passive observer for ships with adaptive wave filtering," *New Directions in Nonlinear Observer Design (H. Nijmeijer and T. I. Fossen, Eds.)*, Springer-Verlag London Ltd., pp. 113–134, 1999.
- [7] T. I. Fossen, "Nonlinear passive control and observer design for ships," *Modeling, Identification and Control (MIC)*, vol. 21, no. 3, pp. 129–184, 2000.

- [8] G. Torsetnes, J. Jouffroy, and T. I. Fossen, "Nonlinear dynamic positioning of ships with gain-scheduled wave filtering," in *Proc. IEEE Conference on Decision and Control (CDC'04)*, Paradise Iceland, Bahamas, 2004.
- [9] V. Hassani, A. J. Sørensen, and A. M. Pascoal, "Robust dynamic positioning of offshore vessels using mixed- μ synthesis, part I: Designing process," in *Proc. ACOOG 2012 - IFAC Workshop on Automatic Control in Offshore Oil and Gas Production*, Trondheim, Norway, 2012.
- [10] —, "Robust dynamic positioning of offshore vessels using mixed- μ synthesis, part II: Simulation and experimental results," in *Proc. ACOOG 2012 - IFAC Workshop on Automatic Control in Offshore Oil and Gas Production*, Trondheim, Norway, 2012.
- [11] E. A. Tannuri, L. K. Kubota, and C. P. Pesce, "Adaptive techniques applied to offshore dynamic positioning systems," *Journal of the Brazilian Society of Mechanical Sciences and Engineering*, vol. 28, no. 3, pp. 323–330, 2006.
- [12] T. D. Nguyen, A. J. Sørensen, and S. T. Quek, "Design of hybrid controller for dynamic positioning from calm to extreme sea conditions," *Automatica*, vol. 43, no. 5, pp. 768–785, 2007.
- [13] A. J. Sørensen, "Structural issues in the design and operation of marine control systems," *Annual Reviews in Control*, vol. 29, pp. 125–149, 2005.
- [14] —, "A survey of dynamic positioning control systems," *Annual Reviews in Control*, vol. 35, pp. 123–136, 2011.
- [15] V. Hassani, J. Hespanha, M. Athans, and A. M. Pascoal, "Stability analysis of robust multiple model adaptive control," in *Proc. of The 18th IFAC World Congress*, Milan, Italy, 2011.
- [16] V. Hassani, A. J. Sørensen, and A. M. Pascoal, "Multiple model adaptive wave filtering for dynamic positioning of marine vessels," in *Proc. ACC'12 - American Control Conference*, Montreal, Canada, 2012.
- [17] G. J. Balas, "mixed- μ software (unpublished version)," 2009, private communication.
- [18] T. I. Fossen and J. P. Strand, "Passive nonlinear observer design for ships using Lyapunov methods: Full-scale experiments with a supply vessel," *Automatica*, vol. 35, pp. 3–16, 1999.
- [19] A. J. Sørensen, "Lecture notes on marine control systems," Norwegian University of Science and Technology, Tech. Rep. Report UK-11-76, 2011.
- [20] V. Hassani, A. J. Sørensen, A. M. Pascoal, and A. P. Aguiar, "Developing a linear model for wave filtering and dynamic positioning," in *Proc. CONTROL012 - the 10th Portuguese Conference on Automatic Control*, Madeira, Portugal, 2012.
- [21] T. I. Fossen, *Handbook of Marine Craft Hydrodynamics and Motion Control*. Chichester, UK: John Wiley & Sons, Ltd, 2011.
- [22] W. G. Price and R. E. D. Bishop, *Probabilistic Theory of Ship Dynamics*. London, UK: Chapman and Hall, 1974.
- [23] S. Skogestad and I. Postlethwaite, *Multivariable Feedback Control: Analysis and Design (2nd Edition)*. Wiley, 2006.
- [24] V. Hassani, A. J. Sørensen, and A. M. Pascoal, "Evaluation of three dynamic ship positioning controllers: from calm to extreme conditions," in *Proc. NGCUV 2012 - IFAC Workshop on Navigation, Guidance and Control of Underwater Vehicles*, Porto, Portugal, 2012.
- [25] S. Fekri, M. Athans, and A. Pascoal, "Issues, progress and new results in robust adaptive control," *Int. J. of Adaptive Control and Signal Processing*, vol. 20, pp. 519–579, 2006.
- [26] B. D. O. Anderson and J. B. Moore, *Optimal Filtering*. New Jersey, USA: Prentice-Hall, 1979.
- [27] A. J. Sørensen, E. Pedersen, and O. Smogeli, "Simulation-based design and testing of dynamically positioned marine vessels," in *Proc. of International Conference on Marine Simulation and Ship Maneuverability (MARSIM'03)*, Kanazawa, Japan, 2003.
- [28] T. I. Fossen and T. Perez, "Marine systems simulator (MSS)," "www.marinecontrol.org", 2009.
- [29] K. Hasselmann, T. P. Barnett, E. Bouws, H. Carlson, D. Cartwright, K. Enke, J. A. Ewing, H. Gienapp, D. E. Hasselmann, P. Kruseman, A. Meerburg, P. Müller, D. J. Olbers, K. Richter, W. Sell, and H. Walden, "Measurements of wind-wave growth and swell decay during the joint north sea wave project (JONSWAP)," *Ergänzungsheft zur Deutschen Hydrographischen Zeitschrift Reihe*, vol. 8, no. 12, pp. 1–95, 1973.